

Exciton diamagnetic shifts in GaAs–Ga_{1–x}Al_xAs quantum dots and ultrathin quantum wells

Z Barticevic¹, M Pacheco¹, C A Duque² and L E Oliveira³

¹ Departamento de Física, Universidad Técnica Federico Santa María, Casilla 110-V, Valparaíso, Chile

² Instituto de Física, Universidad de Antioquia, AA 1226, Medellín, Colombia

³ Instituto de Física, Unicamp, CP 6165, Campinas-SP, 13083-970, Brazil

Received 10 January 2007, in final form 26 March 2007

Published 2 May 2007

Online at stacks.iop.org/JPhysCM/19/216224

Abstract

A theoretical study of the growth-direction magnetic-field effects on the exciton photoluminescence peak energies in GaAs–Ga_{1–x}Al_xAs quantum-dot/ultrathin quantum-well systems is presented. Calculations are performed within the effective-mass approximation and taking into account nonparabolicity effects for both the conduction-band and valence-band effective masses. We use a simple ‘QD + ultrathin QW’ model heterostructure to mimic the actual physical system, and calculated results for the exciton diamagnetic shifts are found in overall agreement with recent experimental measurements.

1. Introduction

The physics of low-dimensional nanosized semiconductor heterostructures has attracted considerable attention in the last two decades or so. This is due to a number of interesting confinement and quantization effects which may introduce modifications in the electronic and optical properties of these semiconductor systems, with the obvious implication of a variety of applications in optoelectronic and spintronic devices. In particular, semiconductor quantum dots (QDs) have been largely used as models for the study of both fundamental electronic properties as well as for coherent optical manipulation of QD states [1–10]. For a number of reasons, GaAs–Ga_{1–x}Al_xAs systems have been the most studied among the low-dimensional semiconductor heterostructures. Here we are concerned with GaAs–Ga_{1–x}Al_xAs QDs and ultrathin quantum wells (QWs). As is well known, these semiconductor systems have almost perfect match of lattice parameters, and sharp interfaces between the two materials may be obtained with reduced intermixing, with the result of ideally unstrained heterostructure systems. Moreover, GaAs QDs may naturally occur at thickness fluctuations of thin GaAs–Ga_{1–x}Al_xAs QWs, which produce a three-dimensional (3D) confinement. Recently, Rastelli *et al* [11] have been able to obtain 3D unstrained GaAs–Ga_{1–x}Al_xAs QDs via hierarchical self-assembly, by combining solid-source molecular beam epitaxy and atomic-layer precise *in situ* etching. They were able to obtain photoluminescence (PL) spectroscopy measurements with very narrow

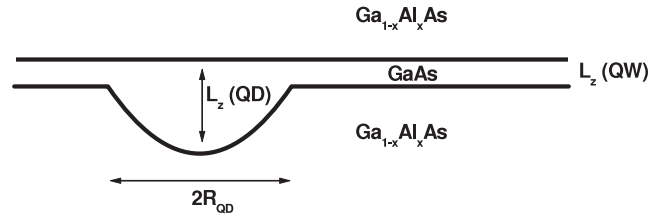


Figure 1. Pictorial view of the ‘QD + ultrathin QW’ model heterostructure used in the present work.

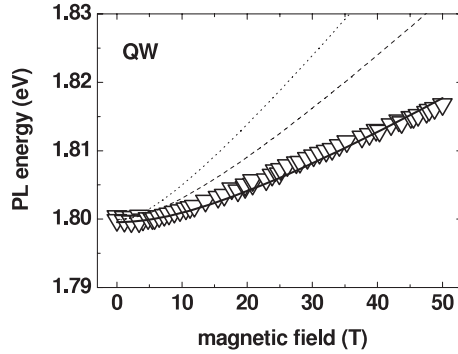


Figure 2. Growth-direction magnetic-field dependence of the heavy-hole exciton peak energies (or ground-state-correlated e–h transition energies) for a symmetric ultrathin $L_z(\text{QW}) = 1.6$ nm GaAs–Ga_{0.65}Al_{0.35}As QW. Experimental data (down triangles) are from Schildermans *et al* [12] and present theoretical results (full curve) are obtained by taking into account nonparabolicity effects for the GaAs conduction [20] band, i.e., $m_e = 0.10 m_0$, where m_0 is the free-electron mass, and for the GaAs valence band [23, 24], with $m_{\text{hh}\parallel} = 0.35 m_0$. For comparison, the dotted line represents our calculated results for an $L_z = 1.8$ nm ultrathin well as in table 1 of Schildermans *et al* [12], with masses in the parabolic-band [18] approximation given as $m_e = 0.0665 m_0$ and $m_{\text{hh}\parallel} = 0.116 m_0$, whereas the dashed curve corresponds to theoretical results for an $L_z = 1.6$ nm well, with $m_e = 0.10 m_0$ and $m_{\text{hh}\parallel} = 0.116 m_0$.

inhomogeneous broadening and clearly resolved excited states at high excitation intensities of 145 W cm^{-2} , and their work was followed by further studies of the optical properties of unstrained GaAs–Ga_{1–x}Al_xAs QD/ultrathin-QW systems [12, 13]. By using simple modelling of the effects of the growth-direction applied magnetic field, Schildermans *et al* [12] estimated the effective exciton mass, and found it to be more than twice the value for bulk GaAs.

The purpose of the present work is to theoretically study the growth-direction magnetic-field effects on the exciton states in GaAs–Ga_{1–x}Al_xAs QDs and ultrathin QWs, and compare calculated results with the measurements by Schildermans *et al* [12] and Sidor *et al* [13]. We first note that magneto-photoluminescence data by Schildermans *et al* [12] in GaAs–Ga_{1–x}Al_xAs QD/ultrathin QW systems reveal well-resolved QW and QD PL peak energies. We choose therefore a simple theoretical modelling⁴ of the GaAs–Ga_{1–x}Al_xAs semiconductor heterostructure which is loosely depicted in figure 1, and should be compared with the insets in figure 2 of Rastelli *et al* [11] or in figure 1 of Schildermans *et al* [12]. In

⁴ In order to simplify the calculations, we choose to model the GaAs–Ga_{1–x}Al_xAs QD/ultrathin-QW systems used in the studies by Rastelli *et al* [11] and Schildermans *et al* [12] by considering both barriers as Ga_{0.65}Al_{0.35}As infinite layers. Note that the heterostructure used in the experimental measurements [11, 12] consisted of a Ga_{0.55}Al_{0.45}As layer and a Ga_{0.65}Al_{0.35}As barrier on the opposite sides of the thin GaAs layer.

the present calculations, we follow Schildermans *et al* [12], who commented that the Zeeman splitting is quite small and the maximum PL shift (occurring at 50 T) due to low-energy spin polarization is found to be 2.5 meV (1.5 meV) for the QWs (QDs) in their experiments [11, 12]. Here, therefore, we ignore spin effects. Moreover, we assume that the relative motion of the carriers and that of the centre of mass (CM) are independent (we note that, strictly, one may only make this separation in the plane of the well [14]). With these assumptions, the exciton envelope wavefunction may be taken as $\Psi_{\text{exc}}(\vec{\rho}, z_e, z_h)$, which depends on the e–h relative coordinates $\vec{\rho} = (\rho, \phi)$ for motion parallel to the heterostructure interfaces and on carrier coordinates z_e and z_h along the growth direction. The work is organized as follows. Section 2 briefly describes the theoretical approach of the present study, section 3 presents results and discussion, and conclusions are given in section 4.

2. Theoretical framework

In the calculation of exciton PL peak energies (or electron–hole (e–h) correlated transition energies) in GaAs–(Ga, Al)As semiconductor QDs, we consider the Hamiltonian [15–17]

$$H = H_e + H_h + V_{\text{QD}} + V_C, \quad (1)$$

where we take into account growth-direction applied magnetic-field effects, i.e., the electron and hole Hamiltonian operators are given as

$$H_e = -\frac{\hbar^2}{2m_e^*} \frac{\partial^2}{\partial z_e^2} + \frac{1}{2m_e^*} \left[-i\hbar(\nabla_e)_\parallel + \frac{e}{c}\mathbf{A}_e \right]^2, \quad (2)$$

$$H_h = -\frac{\hbar^2}{2m_{h_\perp}^*} \frac{\partial^2}{\partial z_h^2} + \frac{1}{2m_{h_\parallel}^*} \left[-i\hbar(\nabla_h)_\parallel - \frac{e}{c}\mathbf{A}_h \right]^2, \quad (3)$$

respectively, where m_e^* is the isotropic electron effective mass, and $m_{h_\perp}^*$ and $m_{h_\parallel}^*$ are the hole effective masses [18]. The V_{QD} confinement potential of the QD is given by

$$V_{\text{QD}} = V_e(z_e) + V_h(z_h) + V_\rho, \quad (4)$$

i.e., it is modelled by the sum of electron and hole one-dimensional z -direction L_z (QD) square-well barrier potentials and a lateral in-plane parabolic confinement potential taken as

$$V_\rho = \frac{1}{2}\mu_x\omega^2\rho^2, \quad (5)$$

where $\mu_x = \frac{m_e^*m_{h_\parallel}^*}{m_e^*+m_{h_\parallel}^*}$ is the heavy-hole exciton in-plane effective mass, $\hbar\omega$ is a measure of the strength of the in-plane confinement potential, and ρ is the e–h in-plane coordinate (it is convenient to define a lateral QD radius as $R_{\text{QD}} = \sqrt{\hbar/\mu_x\omega}$). The e–h correlation is taken into account through

$$V_C = -\frac{e^2}{\epsilon r}, \quad (6)$$

i.e., a Coulomb potential screened by the dielectric constants of the barrier or well materials, where r is the e–h distance.

In order to calculate the QW exciton PL peak energies for an ultrathin QW, we ignore the QD (see figure 1) and consider a thin isolated QW, with $H = H_e + H_h + V_{\text{QW}} + V_C$, and the electron and hole confinements in the z -direction modelled by the L_z (QW) square-well $V_e(z_e)$ and $V_h(z_h)$ barrier potentials $V_{\text{QW}} = V_e + V_h$, respectively. In the above equations, the vector potential is chosen in the symmetric gauge as $\mathbf{A} = (B/2)(-y, x, 0)$. The z -dependent $V_i(z_i)$ ($i = e, h$) confinement potential is invariant under the transformation $z \rightarrow -z$. Therefore, one may assign a definite parity for the e or h QW wavefunction. As the e–h Coulomb

interaction is invariant under the simultaneous inversion of the electron and hole positions, the exciton envelope wavefunction will therefore have a well-defined parity (i.e., parity is a good quantum number), and the excitonic envelope function may be expanded as products of QW electron and hole eigenfunctions preserving the parity. One then may write the exciton envelope wavefunction as

$$\Psi_{\text{exc}}^{\pm}(\vec{\rho}, z_e, z_h) = \sum_{P, P'} \sum_{n_e(P), n_h(P')} B^{n_e(P), n_h(P'), (\pm)}(\vec{\rho}) f_{n_e(P)}(z_e) f_{n_h(P')}(z_h) \Delta_{P, P'}, \quad (7)$$

where P, P' indicate even or odd parity, and $\Delta_{P, P'} = \delta_{P, P'}$ for even (+) excitonic states, whereas $\Delta_{P, P'} = (1 - \delta_{P, P'})$ for odd (-) states. In the above, $f_{n_e(P)}(z_e)$ and $f_{n_h(P')}(z_h)$ are the QW electron and hole eigensolutions, respectively. One, therefore, obtains the following eigenvalue equation for $B^{n_e(P), n_h(P), (+)}(\rho, \theta)$ (and a similar equation for the (-) solution):

$$\left[-\frac{\hbar^2}{2\mu_x} \nabla_{\rho}^2 + \frac{1}{2} \mu_x \omega_{\text{eff}}^2 \rho^2 + \frac{eB}{2c} \left(\frac{1}{m_e^*} - \frac{1}{m_h^*} \right) L_z - \varepsilon(n_e(P), n_h(P)) \right] B^{n_e(P), n_h(P), (+)}(\rho, \theta) - \sum_{P'} \sum_{n_e'(P'), n_h'(P')} V_{n_e'(P'), n_h'(P')}^{n_e(P), n_h(P)}(\rho) B^{n_e'(P'), n_h'(P'), (+)}(\rho, \theta) = 0, \quad (8)$$

where

$$\varepsilon(n_e(P), n_h(P)) = E_{\text{exc}} - E_e - E_{\text{hh}} - E_g, \quad (9)$$

E_g is the bulk GaAs energy gap, E_e (E_{hh}) is the first electron (heavy-hole) QD barrier-potential confinement energy, and E_{exc} denotes the excitonic PL peak energy (or correlated e-h transition energy),

$$\omega_{\text{eff}} = \sqrt{\omega^2 + \frac{1}{4}\omega_c^2}, \quad (10)$$

where $\omega_c = \frac{eB}{\mu_x c}$, and

$$V_{n_e'(P'), n_h'(P')}^{n_e(P), n_h(P)}(\rho) = \langle f_{n_e(P)}(z_e) f_{n_h(P)}(z_h) | V_C | f_{n_e'(P')}(z_e) f_{n_h'(P')}(z_h) \rangle. \quad (11)$$

We note that the above matrix element is θ -independent; equation (8) has azimuthal symmetry and, therefore, one may write

$$B^{n_e(P), n_h(P), (+)}(\rho, \theta) = \exp(im\theta) F_{n_e(P), n_h(P)}^{(+, m)}(\rho), \quad (12)$$

i.e., the z -component of the angular momentum is a good quantum number. One then obtains a set of coupled equations for $F_{n_e(P), n_h(P)}^{(+, m)}(\rho)$, which may be solved numerically by expanding $F^{(+, m)}$ in a set of Gaussian-type functions with length parameters λ , chosen in order to cover the physical range of relevant spatial parameters [15]. Further details of the calculation procedure may be found elsewhere [16, 17].

3. Results and discussion

In what follows, relevant material parameters were initially taken, at low temperature, within the parabolic effective-mass approach, as in Li [18]. For simplicity, we have used the GaAs values of the effective masses and dielectric constant throughout the heterostructure. One must, however, take into account the effects of nonparabolicity both in the conduction [19–22] and valence [23, 24] bands, and possible changes in the values of both the GaAs conduction-band electronic effective mass as well as in the GaAs valence-band effective mass. With respect to the effective electron mass at the Γ minimum for a GaAs–Ga_{0.65}Al_{0.35}As QW with widths

$\lesssim 10\text{--}12$ nm, here we mention that theoretical calculations including nonparabolicity effects on the electron effective mass were performed by de Dios-Leyva *et al* [20] and Stadele and Hess [21], and results were found in very good agreement with the experimental measurements by Michels *et al* [22]. In the case of nonparabolicity effects on the GaAs valence-band effective mass, we refer to the theoretical work by Pacheco *et al* [23] and Ekenberg and Altarelli [24], from which one may estimate the ground-state heavy-hole effective mass to be $0.47m_0$ and $0.55m_0$, where m_0 is the free-electron mass, for GaAs QWs of widths equal to 4 nm and 7 nm, respectively. Notice that present calculations for the growth-direction magnetic-field dependence of the heavy-hole exciton peak energies for a symmetric ultrathin $L_z(\text{QW}) = 1.8$ nm GaAs–Ga_{0.65}Al_{0.35}As QW (i.e., with $L_z(\text{QW})$ as in table 1 of Schildermans *et al* [12]), and that do not include nonparabolicity effects (dotted curve in figure 2), show a theoretical magnetic-field dispersion too steep as compared with experimental results by Schildermans *et al* [12] (see also the results represented by the dashed curve, which includes nonparabolicity effects only for the conduction-band mass, through an $m_e = 0.10 m_0$ electron mass). On the other hand, calculations in which the GaAs conduction-band m_e effective mass is chosen by taking into account nonparabolicity effects as calculated by de Dios-Leyva *et al* [20] (i.e., $m_e = 0.10 m_0$ for a QW thickness of 1.6 nm), and with a heavy-hole effective mass chosen⁵ as $m_{\text{hh}\parallel} = 0.35 m_0$, result in a nice agreement with the measured PL exciton peaks by Schildermans *et al* [12], as is apparent from the full theoretical curve in figure 2. Notice, in this case, that the $L_z(\text{QW}) = 1.6$ nm QW width (which is in good agreement with the value of 1.8 nm for the sample 2 in the experiment) was chosen in order to fit the zero magnetic-field experimental result by Schildermans *et al* [12].

Theoretical calculations, with nonparabolicity effects both for the conduction and valence effective masses, are then performed for the magnetic-field dependence of the diamagnetic shifts of the $m = 0$ ground state, and $m = -1$ and -2 excited states of the heavy-hole exciton for a GaAs–Ga_{0.65}Al_{0.35}As QD of thickness $L_z(\text{QD}) = 4.7$ nm and lateral dimension $2R_{\text{QD}} = 16$ nm. Theoretical results are compared, in figure 3, with the experimental measurements by Schildermans *et al* [12] and Sidor *et al* [13]. One notices that the $L_z(\text{QD}) = 4.7$ nm QD thickness is in fair agreement with the 5.96 nm value quoted, for sample 2, in table 1 by Schildermans *et al* [12]. Theoretical results indicate that a choice of $2R_{\text{QD}} = 16$ nm for the lateral size of the QD, or $\hbar\omega = 17.5$ meV ($\hbar\omega = \hbar^2/\mu_x R_{\text{QD}}^2$), provides a quite good description of the experimental diamagnetic-shift data. Here we note that the present zero-field theoretical results for the PL excitonic peaks are 1613 meV ($m = 0$), 1644 meV ($m = -1$) and 1665 meV ($m = -2$), which should be compared with the experimental [12, 13] PL energies of 1620, 1638 and 1650 meV, or with experimental (excitation intensity of 145 W cm^{-2}) measurements of 1607, 1623, and 1642 meV by Rastelli *et al* [11] for a sample supposedly grown in the same way as sample 2 of Schildermans *et al* [12].

Here we note that, in the present calculations, the effects of nonparabolicity were taken into account through the use of appropriate effective masses both for the conduction electrons and valence-band holes. As shown in previous studies [19–24], such effects may be incorporated into the effective masses, and depend on the size of the QW or QD in question. We have used the corresponding electron effective-mass values obtained in the study by de Dios-Leyva *et al* [20], and calculations of the electron effective mass in that work incorporate the effects of the Zeeman splitting and wavefunction penetration. For the valence-band heavy-hole effective mass [23, 24] we have used $m_{\text{hh}\parallel} = 0.35 m_0$.

⁵ Note that this value of the heavy-hole effective mass is of the same order of magnitude as the values inferred from the theoretical studies by Pacheco *et al* [23] and Ekenberg and Altarelli [24], which take into account nonparabolicity effects for the valence-band effective mass.

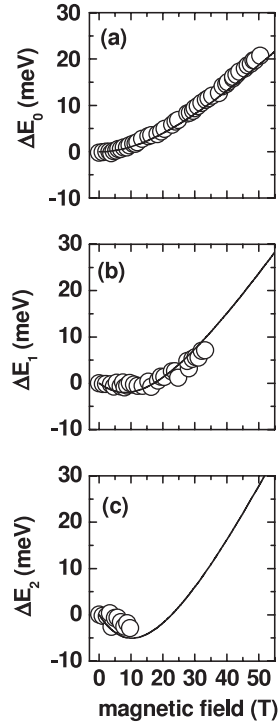


Figure 3. Experimental [12, 13] diamagnetic shifts of the ground state, and first and second excited states of the heavy-hole exciton, in the case of growth-direction applied magnetic fields, for a GaAs–Ga_{0.65}Al_{0.35}As QD, are shown as open dots. Theoretical results for the $m = 0$ ground state, and $m = -1$ and -2 excited states of the heavy-hole exciton are shown as full curves, and calculations are performed for a QD of height/thickness $L_z(\text{QD}) = 4.7$ nm and lateral dimension $2R_{\text{QD}} = 16$ nm, corresponding to an in-plane parabolic $\mu_x \omega^2 \rho^2 / 2$ confinement potential, where μ_x is the heavy-hole exciton effective mass and $\hbar\omega = 17.5$ meV ($\hbar\omega = \hbar^2 / \mu_x R_{\text{QD}}^2$); we take into account nonparabolicity effects for the GaAs conduction [20] band, i.e., $m_e = 0.084 m_0$, where m_0 is the free-electron mass, and for the GaAs valence band [23, 24], with $m_{\text{hh}\parallel} = 0.35 m_0$.

It is of interest to comment that Schildermans *et al* [12] have ‘measured’ the exciton in-plane effective masses through a fitting procedure⁶ of the PL exciton energy, and obtained values two times larger than the bulk GaAs exciton mass. In the present calculation, however, we have obtained agreement with experimental data by including realistically both e–h Coulomb interaction and nonparabolicity effects [20–24] with a conduction-band mass $m_e \approx 0.08\text{--}0.10 m_0$ and a valence-band mass $m_{\text{hh}\parallel} = 0.35 m_0$. This indicates that the values obtained by Schildermans *et al* [12] for the exciton in-plane effective masses should be viewed with caution. The present calculation ignores effects of interdiffusion by taking a QD in-plane confinement-potential profile defined by a lateral QD radius instead of an asymmetric profile as in figures 4(b) and (c) by Rastelli *et al* [11]. We do believe, however, that an isotropic in-plane confinement potential preserves the essential physics of the QD-exciton problem, and that a calculation with a more elaborated profile of the confinement potential would not change the overall conclusions of the present work.

⁶ Here we note that the energy expressions adopted by Schildermans *et al* [12] are oversimplified and do not include, for instance, effects of the e–h Coulomb interaction. We believe this is essentially the reason for obtaining such unrealistic values for the exciton effective mass.

4. Conclusions

Summing up, we have worked within the effective-mass approximation and taken into account nonparabolicity effects for both the conduction and valence effective masses, and performed a theoretical study of the growth-direction magnetic-field effects on the exciton states in GaAs–Ga_{1-x}Al_xAs QDs and ultrathin QWs. Calculated results for the diamagnetic shifts of the $m = 0$ ground state, and $m = -1$ and -2 excited states of the heavy-hole exciton, within a simple ‘QD + ultrathin QW’ model heterostructure, are found in overall agreement with recent experimental measurements by Schildermans *et al* [12] and Sidor *et al* [13].

Acknowledgments

This research was partially supported by Colombian COLCIENCIAS, CODI-Universidad de Antioquia Agencies, and by the Excellence Center for Novel Materials/COLCIENCIAS (contract No. 043-2005). We also acknowledge partial financial support from the Millennium Scientific Initiative/Chile (Condensed Matter Physics, grant P02-054-F), Fondecyt (grants 1061237 and 7060292), Universidad Técnica Federico Santa Maria (internal grant), and Brazilian Agencies CNPq, FAPESP, Rede Nacional de Materiais Nanoestruturados/CNPq, and Millennium Institute for Quantum Computing/MCT.

References

- [1] Stievater T H, Li X, Steel D G, Gammon D, Katzer D S, Park D, Piermarocchi C and Sham L J 2001 *Phys. Rev. Lett.* **87** 133603
Chen G, Stievater T H, Batteh E T, Li X, Steel D G, Gammon D, Katzer D S, Park D and Sham L J 2002 *Phys. Rev. Lett.* **88** 117901
Yuan Z, Kardynal B E, Stevenson R M, Shields A J, Lobo C J, Cooper K, Beattie N S, Ritchie D A and Pepper M 2002 *Science* **295** 102
Zrenner A, Beham E, Stuffer S, Findels F, Bichler M and Abstreiter G 2002 *Nature* **418** 612
Li X, Wu Y, Steel D, Gammon D, Stievater T H, Katzer D S, Park D, Piermarocchi C and Sham L J 2003 *Science* **301** 809 and references therein
- [2] Hours J, Varoutis S, Gallart M, Bloch J, Robert-Philip I, Cavanna A, Abram I, Laruelle F and Gérard J M 2003 *Appl. Phys. Lett.* **82** 2206
- [3] Matsuda K, Saiki T, Nomura S, Mihara M, Aoyagi Y, Nair S and Takagahara T 2003 *Phys. Rev. Lett.* **91** 177401
- [4] Gu J and Liang J-Q 2004 *Phys. Rev. A* **323** 132
- [5] Schulhauser C, Högele A, Govorov A O, Warburton R J, Karrai K, Garcia J M, Gerardot B D and Petroff P M 2004 *Physica E* **25** 233
- [6] Brandi H S, Latgé A and Oliveira L E 2005 *J. Phys.: Condens. Matter* **17** 3665
Brandi H S, Latgé A, Barticevic Z and Oliveira L E 2005 *Solid State Commun.* **135** 386
- [7] Xie W 2005 *Physica B* **358** 109
- [8] Wang G and Guo K 2005 *Physica E* **28** 14
- [9] Karabulut I and Safak H 2005 *Physica B* **368** 82
- [10] Lei W, Chen Y H, Xu B, Jin P, Wang Y L, Zhao Ch and Wang Z G 2006 *Solid State Commun.* **137** 606
- [11] Rastelli A, Stuffer S, Schliwa A, Songmuang R, Manzano C, Constantini G, Kern K, Zrenner A, Bimberg D and Schmidt O G 2004 *Phys. Rev. Lett.* **92** 166104
- [12] Schildermans N, Hayne M, Moshchalkov V V, Rastelli A and Schmidt O G 2005 *Phys. Rev. B* **72** 115312
- [13] Sidor Y, Partoens B, Peeters F M, Schildermans N, Hayne M, Moshchalkov V V, Rastelli A and Schmidt O G 2006 *Phys. Rev. B* **73** 155334
- [14] Bastard G, Mendez E E, Chang L L and Esaki L 1982 *Phys. Rev. B* **26** 1974
Brown J W and Spector H N 1987 *Phys. Rev. B* **35** 3009
- [15] Pacheco M and Barticevic Z 1997 *Phys. Rev. B* **55** 10688
- [16] Pacheco M, Barticevic Z and Claro F 1993 *J. Phys.: Condens. Matter* **5** A363
Barticevic Z, Pacheco M and Claro F 1995 *Phys. Rev. B* **51** 14414
Pacheco M and Barticevic Z 1999 *J. Phys.: Condens. Matter* **11** 1079
Pacheco M and Barticevic Z 2001 *Phys. Rev. B* **64** 033406

-
- [17] Barticevic Z, Pacheco M, Duque C A and Oliveira L E 2002 *J. Appl. Phys.* **92** 1227
Barticevic Z, Pacheco M, Duque C A and Oliveira L E 2003 *Phys. Rev. B* **68** 073312
Duque C A, Porras-Montenegro N, Barticevic Z, Pacheco M and Oliveira L E 2006 *J. Phys.: Condens. Matter* **18** 1877
- [18] Li E H 2000 *Physica E* **5** 215
- [19] de Dios-Leyva M, Reyes-Gómez E, Perdomo-Leiva C A and Oliveira L E 2006 *Phys. Rev. B* **73** 085316
Reyes-Gómez E, Perdomo-Leiva C A, de Dios-Leyva M and Oliveira L E 2006 *Phys. Rev. B* **74** 033314
- [20] de Dios-Leyva M, Porras-Montenegro N, Brandi H S and Oliveira L E 2006 *J. Appl. Phys.* **99** 104303
- [21] Städele M and Hess K 2000 *J. Appl. Phys.* **88** 6945
- [22] Michels J G, Warbuton R J, Nicholas R J, Harris J J and Foxon C T 1993 *Physica B* **184** 159
- [23] Pacheco M, Barticevic Z and Claro F 1992 *Phys. Rev. B* **46** 15200
- [24] Ekenberg U and Altarelli M 1985 *Phys. Rev. B* **32** 3712